

Estimating Long-term Surface Hydrological Components by Coupling Remote Sensing Observation with Surface Flux Model*

by

Jie Song
Department of Geography
Northern Illinois University
DeKalb, Illinois 60115

and

M. L. Wesely
Environmental Research Division
Argonne National Laboratory
Argonne, Illinois 60439

for

Presentation and Lecture Notes Volume
Geoinformatics '2002
Geoinformatics for Global Change Studies and Sustainable Development
CPGIS (The International Association of Chinese Professionals in GIScience)
and Nanjing University
Nanjing, P.R. China, June 1-3, 2002

*Work supported by the U.S. Department of Energy, Office of Science, Office of Biological and Environmental Research, Environmental Sciences Division, under contract W-31-109-Eng-38.

| |
|--|
| <small>The submitted manuscript has been created by the University of Chicago as operator of Argonne National Laboratory under Contract No. W-31-109-ENG-38 with the U.S. Department of Energy. The U.S. government retains for itself, and others acting on its behalf, a paid-up, nonexclusive, irrevocable worldwide license in said article to reproduce, prepare derivative works, distribute copies to the public, and perform publicly and display publicly, by or on behalf of the government.</small> |
|--|

Estimating Long-term Surface Hydrological Components by Coupling Remote Sensing Observation with Surface Flux Model

Jie Song^[1], Marvin L. Wesely^[2]

^[1] Northern Illinois University, DeKalb, IL 60115

^[2] Argonne National Laboratory, Argonne, IL

ABSTRACT

A model framework for parameterized subgrid-scale surface fluxes (PASS) has been applied to use satellite data, models, and routine surface observations to infer root-zone available moisture content and evapotranspiration rate with moderate spatial resolution within Walnut River Watershed in Kansas. Biweekly composite normalized difference vegetative index (NDVI) data are derived from observations by National Oceanic and Atmospheric Administration (NOAA) satellites. Local surface observations provide data on downwelling solar irradiance, air temperature, relative humidity, and wind speed. Surface parameters including roughness length, albedo, surface water conductance, and the ratio of soil heat flux to net radiation are estimated; pixel-specific near-surface meteorological conditions such as air temperature, vapor pressure, and wind speed are adjusted according to local surface forcing. The PASS modeling system makes effective use of satellite data and can be run for large areas for which flux data do not exist and surface meteorological data are available from only a limited number of ground stations. The long-term surface hydrological budget is evaluated using radar-derived precipitation estimates, surface meteorological observations, and satellite data. The modeled hydrological components in the Walnut River Watershed compare well with stream gauge data and observed surface fluxes during 1999.

Keywords: remote sensing, soil moisture, evapotranspiration

1. INTRODUCTION

Evapotranspiration is an essential component of the surface hydrological balance, but obtaining accurate estimates of the surface water vapor flux over large terrestrial areas can be difficult because of the large temporal and spatial variability associated with the unevenness of precipitation and diversity of vegetation. Nevertheless, variations in soil moisture content, groundwater levels, and runoff in streams and rivers cannot be adequately simulated without knowledge of evapotranspiration rates. In the current study, a parameterized subgrid-scale surface flux model (PASS2) (Song et al., 2000a, b) is applied to estimate evapotranspiration after initial estimates of soil moisture are made with PASS1. The goal is to model long-term satellite-pixel-scale moisture and energy fluxes by coupling satellite remote sensing data with a limited set of surface meteorological measurements. Continuous meteorological observations made at the Atmospheric Boundary Layer Experiments (ABLE) site in the Walnut River Watershed (WRW) in Kansas are coupled with daily radar observed precipitation and biweekly composite normalized difference vegetation index (NDVI) to implement PASS2.

Field observations of soil moisture content typically are too limited to provide the spatial resolution and coverage required to describe adequately the spatial heterogeneity of soil moisture over extended areas. Song et al. (1997) modeled the influence of heterogeneous soil moisture on latent and sensible heat fluxes and found that simulated regional-scale latent heat fluxes tend to be higher and air temperatures lower under uniform surface conditions than under spatially heterogeneous conditions. Pitman et al. (1993) demonstrated that possible biases associated with the under-representation of regional land surface heterogeneity within climate models might explain the propensity of climate models to overestimate grid-cell evapotranspiration and underestimate runoff. Hence, detailed information on the spatial distribution of the surface conditions appears to be necessary to simulate evapotranspiration accurately over extended areas. However, estimating surface fluxes at high spatial resolution can be difficult because remote sensing data emphasize local land surface conditions, while the surface fluxes can be strongly influenced by surface-atmosphere interactions occurring over substantially larger areas (Friedl, 1996). PASS2 overcomes these limitations by coupling NDVI from Advanced Very High Resolution Radiometer (AVHRR) satellite data with limited meteorological observations in the study region to infer the surface temperature, root-zone available moisture (RAM) content, and evapotranspiration at satellite pixel resolution.

2. DESCRIPTION OF THE PASS2 MODEL

The PASS2 model, like the original PASS model (Gao, 1995; Gao et al., 1998), uses a rapid algorithm for computing subgrid scale surface energy partitioning on the basis of an analytical solution to surface energy budget equations. A rapid computing algorithm is needed for long-term studies because of the large number of pixels associated with the satellite, land use, and soil characteristics data. Figure 1 provides an outline of the approach. All variables in the model are described either at the subgrid (SG) scale or the model grid (MG) scale, where SG corresponds to the scales of satellite or land use pixels and MG corresponds to scales of at least 100 km. The MG scale variables are approximated by the average of the observations made at the surface meteorological stations. Values of SG surface parameters, including roughness length, surface albedo, surface conductance for water vapor, and the ratio of soil heat flux to net radiation, are estimated by using functional relationships between the surface parameters and satellite-derived spectral indices according to land use classes. These relationships contain empirical coefficients whose values in this study had been derived for midlatitude areas with surface vegetation dominated by grasslands and agricultural crops and might not be suitable for areas with different surface characteristics. Pixel-specific near-surface meteorological conditions such as air temperature, vapor pressure, and wind speed are adjusted according to local surface forcing to account for the feedback of the locally influenced meteorological conditions on the local atmosphere-surface exchange.

a. Step 1, Model Inputs

Data on biweekly composite NDVI or simple ratio SR are obtained along with initial root-zone available moisture (RAM) content θ_a for each pixel i . Arithmetic means of incoming solar irradiance K_{\downarrow} , surface air temperature T_a , relative humidity RH, and wind speed u observed at surface meteorological stations in the area are required to drive the calculations of energy fluxes and RAM content forward in time. Data on land use and available water capacity θ_A necessary for various steps in PASS2 are provided from the soil survey database.

b. Step 2, Precalculation

The precalculation step focuses on estimating pixel-specific surface temperature T_s and the domain-representative surface temperature, both of which are needed to apply the distribution function for T_a in step 3 (Fig. 1). A means of estimating the surface temperature is required because continuous temperature readings from satellite observations are not available. The surface temperatures are estimated in PASS2 with a second-order approximation involving the energy budget equation (Paw U and Gao, 1988; Gao, 1995). The approximation for T_s is used for individual pixels and domain-representative values separately; that is, the latter is not just the arithmetic mean of the former. As Fig. 1 shows, the inputs needed to estimate T_s include several subgrid-scale parameters. The surface albedo α and the ratio Γ of soil heat flux to net radiation are derived from SR and the solar zenith angle for each land use class in the same way as in PASS1. The aerodynamic resistance R_a and its embedded parameter of friction velocity u^* are found with bulk aerodynamic equations using z_0 and u (Song et al., 2000a). Here u at each pixel i is estimated with the wind distribution function, which is shown in Fig. 1. The surface water vapor conductance g_c is found in step 4 except for the first time increment, when the regional average value of the water vapor deficit factor is used because pixel-specific values are not yet available. The incoming longwave radiation is parameterized by water vapor pressure and atmospheric temperature (Satterlund, 1979).

c. Step 3, Subgrid Scale Distribution

Stations for routine meteorological observations are available at coarse spatial resolution, while computation of the surface energy and water budgets require meteorological data at fine resolution. One of the distinct features of the PASS2 model is its spatial redistribution of meteorological information, based in part on procedures described by Seth et al. (1994). Here the regional meteorological variables for wind speed, air temperature, and water vapor pressure are spatially distributed to individual pixels according to surface conditions and the strength of local vertical transfer. The distribution functions shown in step 3 of Fig. 1 are used to find wind speed u for each pixel at a reference height z of about 10 m above the aerodynamic displacement height d and to find air temperature T_a and water vapor pressure e_a at 1.5-2.0 m above the displacement height. These variables are evaluated for each time step throughout the diurnal cycle. The terms α_T and α_E represent surface-atmosphere transfer coefficients (Song et al., 2000a).

d. Step 4, Postcalculation

After the pixel-scale variables are estimated by using the distribution function, g_c is recalculated with pixel-specific vapor deficit values. Important variables in this calculation include SR derived from the most recent satellite data NDVI and photosynthetically active radiation, assumed here to be equal to half of incident solar radiation for each time step. Most importantly, the relative available water content $\Theta = \theta_a / \theta_A$ for each time step is taken into account in estimating the surface conductance.

e. Step 5, Energy Balance

The latent heat flux λE for each pixel is initially estimated using a bulk aerodynamic expression for each pixel. The term δe represents the difference between the saturation vapor pressure at the pixel-specific surface temperature and the ambient air vapor pressure. The sensible heat flux H is likewise initially estimated with a bulk aerodynamic expression. The net radiation R_n is found from the radiation balance involving observed K_{\downarrow} together with the parameterized function for albedo α , incoming longwave irradiance L_{\downarrow} and outgoing longwave irradiance L_{\uparrow} . The initial estimates of λE and H are then adjusted using $R_n(1 - \Gamma)$ as shown in Fig. 1 so that the energy balance is properly closed. This adjustment does not change the Bowen ratio, $H/\lambda E$ and reduces the effects of any poor estimates of aerodynamic resistance in producing potentially unrealistic values.

f. Step 6, Estimates of New θ_a

The decrease in RAM content due to evapotranspiration for each pixel during time increment δt is computed for the root zone (Fig. 1), which is represented by a single layer of soil with depth δz . In principle, increases due to precipitation could also be estimated in this step if adequate precipitation estimates were available (e.g., from calibrated radar data) and if runoff were simulated. The root-zone depth is a crucial variable, but is quite difficult to estimate accurately because it is dependent on plant species and the stage of growth, which are not identified well on the basis of the information available to PASS2. That is, only broad categories of vegetation are identified, and only the general state of the vegetation can be inferred on the basis of SR data from satellites. This version of PASS2 assumes that δz is equal to one-third of canopy height h for croplands, where h is estimated as $10z_0$; 0.2 m for rangeland; 2 m for woodland; and 0.2 m for residential- and urban-related grassy areas. These values account for all of important land use classes (Song et al., 2000a). The depths might be too small to include the entire root zone of the vegetation, but they include the majority of the roots (e.g., Jackson et al., 1996). Because water extraction at the greater depths can be important when the moisture in the upper layers becomes depleted, this version of PASS2 might underestimate evapotranspiration for dry conditions. Steps 1-6 are repeated for each time increment after the set of θ_a values produced by step 6 is supplied as an input to step 1. The amounts of water loss by evapotranspiration can be summed over long periods of time and used in hydrological moisture budgets. PASS2 assumes that excessive soil water after heavy rainfall produces runoff.

3. MODEL APPLICATION

The WRW covers an area of approximately 5000 km² east of Wichita, Kansas (Fig. 2). It is located in the Arkansas-Red River Basin and is enclosed by the southern Great Plains Clouds and Radiation Testbed of the U.S. Department of Energy's Atmospheric Radiation Measurement (ARM) program. The dominate land uses are grassland in the eastern WRW and cropland in the west. Urban areas are scattered, with Wichita on the western edge of the WRW.

Measurements of solar radiation and routine meteorological variables, such as wind, temperature and humidity, are continuously conducted and recorded at 30-min intervals at the ABLE site (Fig. 3). The PASS model has been tested and evaluated during the intensive observation period operated by the Cooperative Atmosphere-Surface Exchange Study during April and May 1997 (Song et al., 2000b). It is found that PASS model can simulate latent and sensible heat fluxes well over a wide range of surface conditions occurred during the early growing season. In addition to radiation and meteorological observations, the effects of spatial variations in precipitation and vegetation cover have to be considered for simulations over longer period of time. Daily total precipitation data at 4-km resolution are obtained from radar measurements. Bi-weekly NDVI composite data obtained from AVHRR data at 1-km resolution are used to update the vegetation change with seasonal changes (Fig. 4).

Simulations of evapotranspiration during 1999 are conducted using PASS2, in which meteorological data are coupled with satellite observations. The time step is 30 min, which correspond to the recorded time intervals for the radiation and meteorological data. Because the land use and available water capacity data are at a resolution of 200 m, while AVHRR data are at 1 km and precipitation data are at 4 km, the effects of merging different spatial resolution data into the model has been investigated. Model simulations are performed at 200-m and 1-km resolutions in year 1999. For 200-m resolution simulation, the coarse resolution data on NDVI and precipitation are assigned to the enclosed fine grid cells. For 1-km resolution simulation, the dominant land use type within each 1-km grid cell is chosen, whereas the values of available water capacity are averaged within each 1-km grid cell. Likewise, the coarser precipitation data are assigned to the finer 1-km grid. It is found that results of model simulation at 1-km resolution are almost the same as at 200-m resolution; the difference in total simulated evapotranspiration values in 1999 is insignificant. Two possible reasons are: (a) under the same meteorological conditions, the surface evapotranspiration is sensitive to the spatial distributions of vegetation density and precipitation, which are simulated at relatively coarse resolution, and not highly sensitive to land use type and available water capacity, which are simulated at finer resolution; and (b) the simulated spatial variations in land use and available water capacity are relatively small in the WRW, so that 1-km

spatial resolution appears adequate to capture the major variations. Because the spatial distributions of land use and available water capacity at finer resolution are constant with time, it is expected that model simulations over other time period at 200-m or 1-km resolutions would obtain similar results.

The accumulative values of simulated evapotranspiration and the observed precipitation and runoff for the entire WRW are displayed in Fig. 5, along with modeled variations in watershed mean soil root-zone moisture computed every 30 min. In comparison with observed soil moisture at 5-cm depth at a energy flux site where prairie grass dominates in the WRW, the simulated mean soil root-zone moisture agrees well with observed values over the year, with both lowest values occurring around the 250th day of the year. In comparison with evapotranspiration observed at the energy flux site, the accumulative rates of evapotranspiration simulated over the whole watershed agrees well with the observations. The difference between the radar-observed precipitation and the sum of PASS2-simulated evapotranspiration and measured runoff for the entire WRW is a relatively small positive value at the end of the year-long simulation period. The differences might be associated with (a) the annual variation in the groundwater recharge, (b) observational errors in radar precipitation, (c) inaccurate precipitation values at the watershed boundary due to the coarse precipitation resolution, (d) inclusion of more watershed areas at the watershed boundary due to the coarse model grid cell, and (e) errors in model simulation due to simplified parameterization schemes and assumed root-zone depths.

4. SUMMARY

Continuous, conventional surface meteorological observations and occasional satellite observations at detailed spatial resolution are coupled by the PASS2 model to produce estimates of surface evapotranspiration at the WRW in the Great Plains of the United States. The long-term simulation of evapotranspiration is used with observed precipitation and runoff to evaluate the surface hydrological balance. Despite its the simplicity of the treatment of root-zone depth and runoff and its highly parameterized description of processes, the current version of PASS2 evapotranspiration and root-zone moisture can be simulated reasonably well and efficiently over the heterogeneous surfaces of the WRW. The effective merging of the data sets of different spatial resolutions to 1 km requires less computation and yet does not produce significant discrepancies in the simulated water budget. Further work is required to consider (a) evaporation from leaf intercepted precipitation, (b) water percolating into the deeper soil below the root-zone depth, and (c) groundwater recharge.

Acknowledgements. This work was supported by the U.S. Department of Energy, Office of Science, Office of Biological and Environmental Research, Environmental Science Division, Water Cycle Pilot Study, under contract W-31-109-Eng-38 to Argonne National Laboratory. Some of the analysis of data was supported by U.S. Department of Energy's ARM program.

References

- Friedl, M. A., 1996, Relationships among remotely sensed data, surface energy balance, and area-averaged fluxes over partially vegetated land surfaces. *Journal of Applied Meteorology*, **35**, 2091-2103.
- Gao, W., 1995, Parameterization of subgrid-scale land surface fluxes with emphasis on distributing mean atmospheric forcing and using satellite-derived vegetation index. *Journal of Geophysical Research*, **100**, 14305-14317.
- Gao, W., R. L. Coulter, B. M. Lesht, J. Qiu, and M. L. Wesely, 1998, Estimating clear-sky regional surface fluxes in the southern Great Plains Atmospheric Radiation Measurement site with ground measurements and satellite observations. *Journal of Applied Meteorology*, **37**, 5-22.
- Paw U, K. T., and W. Gao, 1988, Application of solutions to nonlinear energy budget equations. *Agriculture and Forest Meteorology*, **43**, 121-145.
- Pitman, A. J., Z. L. Yang, and A. Henderson-Sellers, 1993: Subgrid scale precipitation in AGCMs: Re-assessing the land surface sensitivity using a single column model. *Climate Dynamics*, **9**, 33-41.
- Satterlund, D. R., 1979, An improved equation for estimating long-wave radiation from the atmosphere. *Water Resource Research*, **15**, 1649-1650.

Seth, A., F. Giorgi, and R. E. Dickinson, 1994, Simulating fluxes from heterogeneous land surfaces: Explicit subgrid method employing the biosphere-atmosphere transfer scheme (BATs). *Journal of Geophysical Research*, **99**, 18651-18667.

Song, J., C. J. Willmott, and B. Hanson, 1997, Influence of heterogeneous land surfaces on surface energy and mass fluxes. *Theory and Applied Climatology*, **58**, 175-188.

Song J., M.L. Wesely, R.L. Coulter, and E.A. Brandes, 2000a, "Estimating watershed evapotranspiration with PASS. Part I: inferring root-zone moisture conditions using satellite data." *Journal of Hydrometeorology*, **1**, 447-461.

Song J., M.L. Wesely, M.A. LeMone, and R.L. Grossman, 2000b, Estimating watershed evapotranspiration with PASS. Part II: moisture budgets during drydown periods. *Journal of Hydrometeorology*, **1**, 462-473.

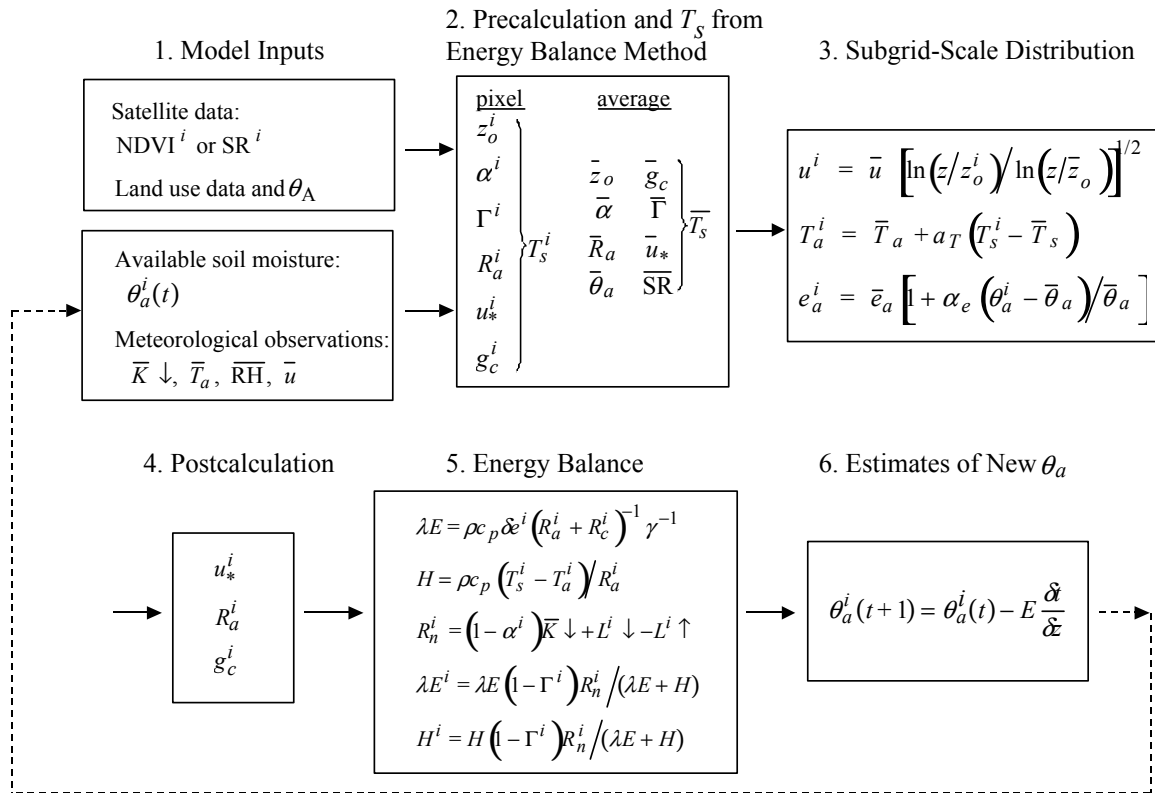


Fig.1. Scheme of PASS2 model.

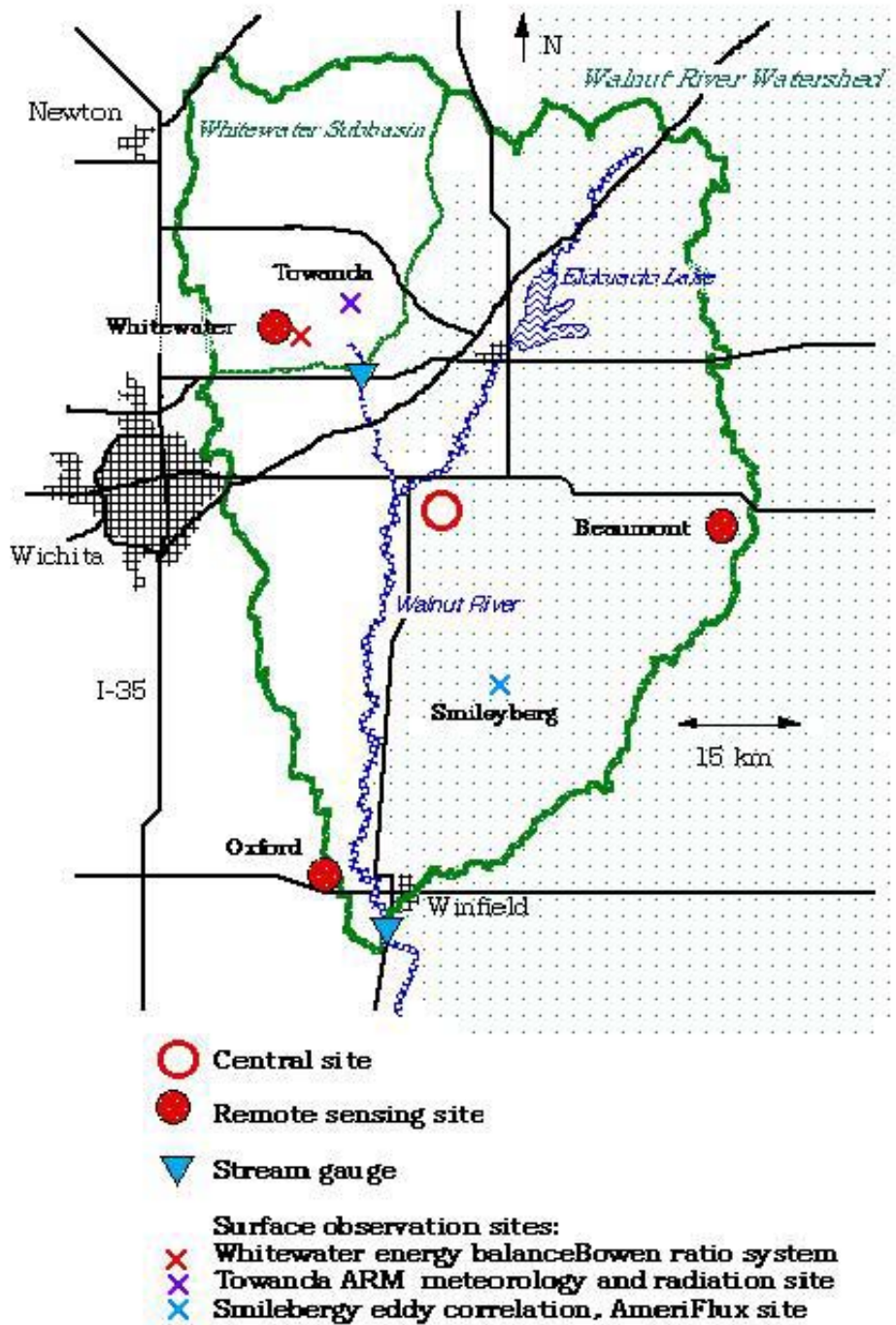


Fig. 2. Atmospheric Boundary Layer Experiment facilities at the Walnut River Watershed.

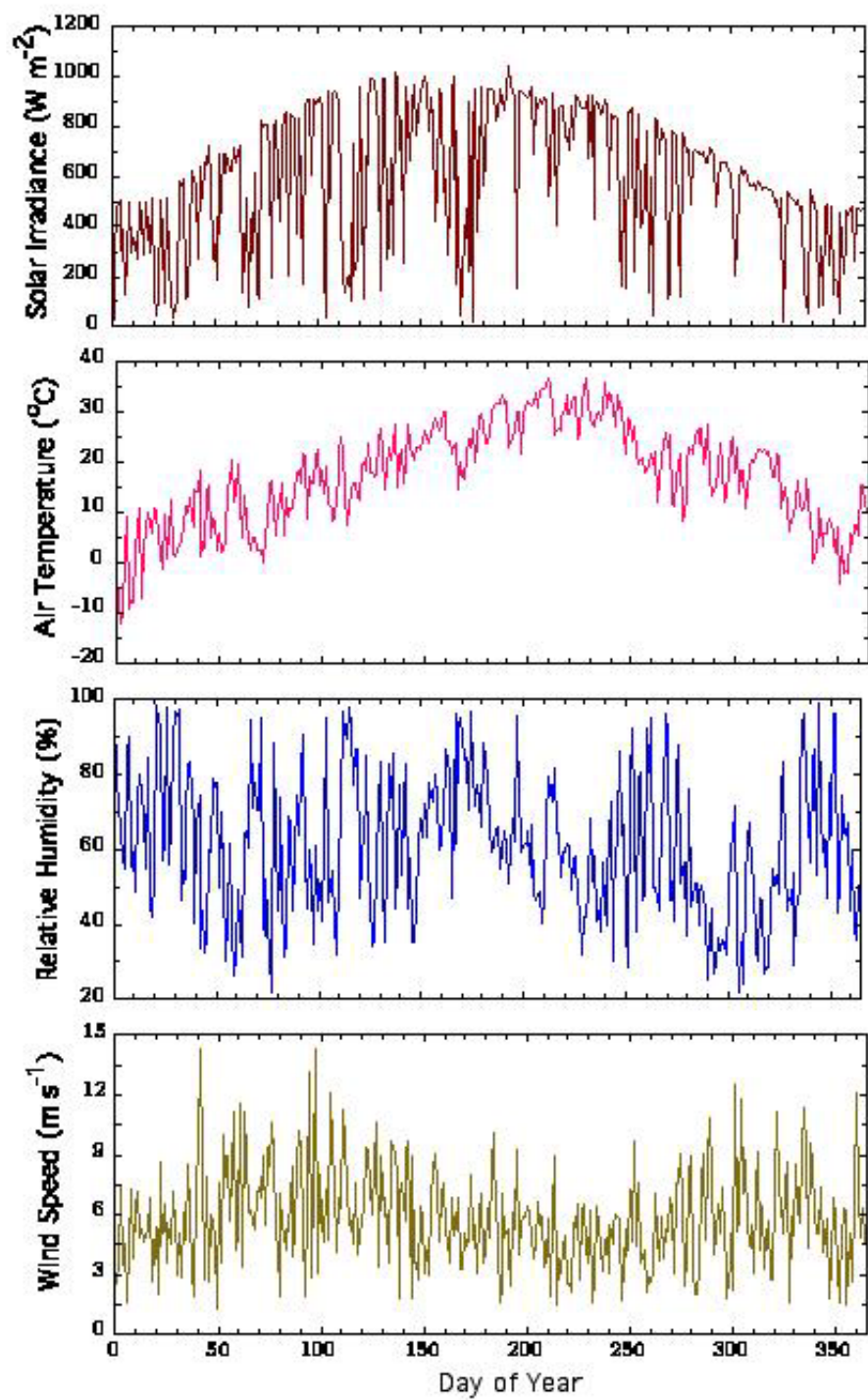


Fig. 3. Solar radiation and routine meteorological observations during year 1999, with noon time values displayed.

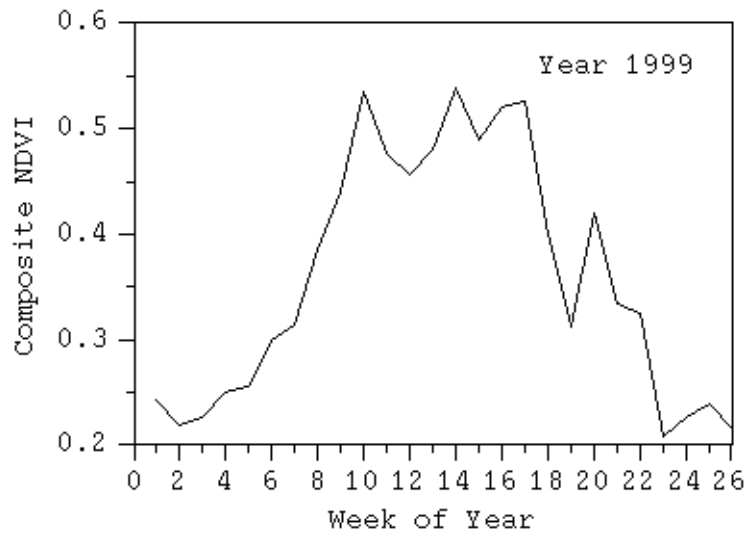


Fig. 4. Biweekly composite NDVI averaged over WRW during 1999.

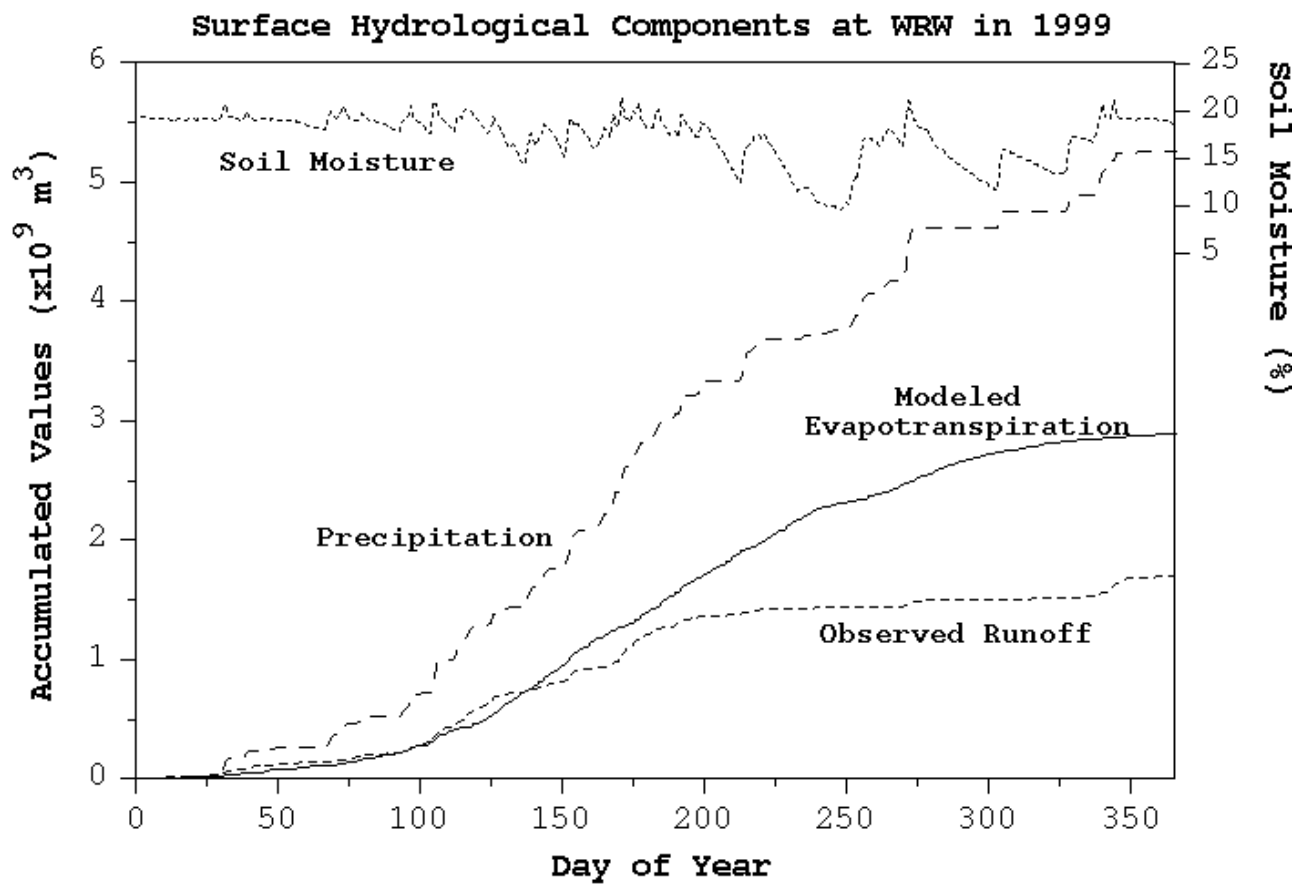


Fig. 5. Accumulative evapotranspiration estimates over WRW during 1999.